18th Australasian Fluid Mechanics Conference
Launceston, Australia
3-7 December 2012

Comparison of fluid forces and wake modes between free vibration and tracking motion of a circular cylinder

J. Zhao[1], A. Nemes[1], D. Lo Jacono[1,2,3] and J. Sheridan[1]

[1]Fluids Laboratory for Aeronautical and Industrial Research (FLAIR)
Department of Mechanical and Aerospace Engineering
Monash University, Melbourne, Victoria, 3800 Australia

[2]Université de Toulouse; INPT, UPS; IMFT;
Allée Camille Soula, F-31400 Toulouse, France

[3]CNRS; IMFT; F-31400 Toulouse, France

Abstract

In this study, experimental investigation compares the fluid forces and wake modes of a freely-vibrating circular cylinder and a VIV-trajectory-tracking cylinder. The free VIV response was modelled on a low-friction air bearing system in conjunction with water channel facilities exhibits classical three amplitude-response ("initial", "upper" and "lower") branches. Measurements of the fluid forces, cylinder displacement and the wake modes are simultaneously conducted. On the other hand, the forced vibration experiments were conducted using a real-time PID motion controller with very high accuracy. Compared to the previous work of a cylinder undergoing sinusoidally-driven oscillations, the present study provides a more accurate comparison between free and forced vibrations. The wake modes of the cylinder undergoing tracking motion show some remarkable similarities to the case of free vibration.

Introduction

Vortex-induced vibration (VIV) of a circular cylinder has been intensively studied in the past few decades, due to its undesired impact on the fatigue life of structures, which can potentially lead to structural damage or catastrophic failure. This is critical in many engineering applications, such as flow around offshore oil production risers, civil buildings and bridges. Extensive work has been motivated and undertaken in the past, which is well covered in collections by [2, 18].

To understand the fundamentals of VIV of a circular cylinder, the fluid-structure system has been simplified as a linear mass-spring-damper system in particular with one degree of freedom in the cross-flow direction. The dynamics of cross-flow VIV of a cylinder is mathematically represented by the following differential equation of motion:

$$m\ddot{y} + c\dot{y} + ky = F_y, \tag{1}$$

where m is the system's mass, c is the structural damping, k is the spring constant, y is the cylinder's time-varying displacement, and F_y is the instantaneous fluid lift force acting on the cylinder in the direction transverse to the free-stream. A definition schematic diagram of cross-flow VIV of a rigid smooth circular cylinder is given in figure 1.

A pioneering experimental study in a wind tunnel by Feng [5] characterised the vibration amplitude and frequency responses of a circular cylinder at high mass ratios of $m^* = m/m_d \approx O(100)$, where m is the system mass and m_d is the displaced fluid (air) mass by the cylinder, over a range of reduced velocities, $U^* = U/f_N D$, where U is the free-stream velocity, f_N is the natural frequency of system measured in the still fluid. Feng found that the cylinder experiences largest oscillation amplitudes in a synchronisation region where the vortex shedding

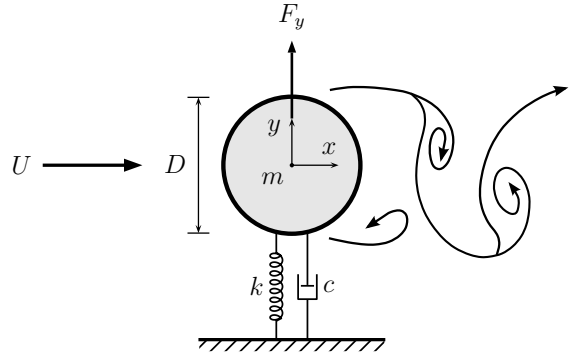

Figure 1: Definition sketches for cross-flow VIV of a circular cylinder. The cylinders are allowed to oscillate freely only in the transverse direction y, to the oncoming flow U in the streamwise direction x. Note that characteristic length is the frontal projected lengths of the cross section, the cylinder diameter.

frequency (f_s) locks on to the cylinder's oscillating frequency (f), and both frequencies are close to the natural frequency of the system (f_N): $f_s \cong f \cong f_N$. More recent experiments of a cylinder at low mass ratios ($m^* \approx O(1)$) in water channel conducted by Khalak and Williamson [10, 11, 13] showed that a distinct three-branch (termed by the "initial", the "upper" and the "lower" branches) amplitude response occurs over a reduced velocity range, which was not observed in case of high mass ratios by Feng. Compared to Feng's experiments, they also found that the oscillation amplitudes are much larger with the "lock-in" region extended to much higher reduced velocities, and that within the "lock-in" region the normalised oscillation frequency $f^* = f/f_N$ is larger than unity and increases monotonically with the reduced velocity. Further experiments by [8, 15] found that magnitude of the peak amplitude is influenced not only by the parameters of mass and damping ratios but also by Reynolds number, defined as $\mathrm{Re} = UD/\nu$, where ν is the kinematic viscosity of the fluid. Experiments [7] have shown that the wake in the initial branch consists of two single vortices shed in one oscillation cycle (2S mode), while the upper and lower branches are associated with two pairs of vortices being shed in one oscillation cycle (2P mode).

In order to better understand and then to predict the response of free vibrations, researchers have employed cylinders undergoing forced sinusoidal oscillations as a complementary model, by decoupling the fluid-structure interaction, to simplify the problems of VIV [1, 4, 16, 17, 19], simply because the results of free vibrations have shown that the cylinder motion and the lift force in the lock-in region are well represented by sinusoidal functions [5, 7, 11]. Comparisons between the free and forced

vibration cases in the literature have shown that although both cases exhibit many characteristic similarities in the wake modes and fluid forcing, there still exist major differences in energy transfer between the fluid and the structure [4, 16]. Therefore, the question still remains unaddressed whether precise forced vibration following the trajectories of the free vibration case can reproduce the same fluid forces and wake modes.

The present study provides a direct comparison of the dynamic response and wake modes between a freely-vibration cylinder and a VIV-trajectory-tracking cylinder. The experimental details, the results and conclusions will be presented in the following sections.

Experimental Details

The experiments were conducted in the free-surface recirculating water channel of FLAIR in the Department of Mechanical and Aerospace Engineering at Monash University. The water channel facility has a test section of 4000mm in length, 600mm in width and 800mm in depth.

For the free VIV experiments, a rigid circular cylinder was vertically mounted on a low-friction air bearing system which was placed on top of the water channel, allowing linear oscillatory movement of the cylinder transverse to the free-stream. The cylinder used was made from carbon fibre tubes having an outside diameter of $D = 25$mm and a wall thickness of 1.5mm. The immersed length of the body was $L = 620$mm, giving an aspect ratio of $L/D = 24.8$ and a displaced water mass of $m_d = \pi D^2 L/4 = 306.2$g. The body movement was elastically constrained by a pair of extension springs (LE014B13S, Lee Spring). The total mass of the oscillating system was $m = 813.2$g, resulting in a mass ratio of $m^* = m/m_d = 2.66$. To promote parallel vortex shedding, the end condition of the body was controlled using a platform (with a 500×500mm^2 top plate and 165mm in height) placed on the water channel floor, giving a gap of approximately 2mm between the cylinder's free end and the platform. Free decay tests were conducted individually in air and quiescent water to measure the natural frequencies of the system, $f_{na} = 0.874$Hz in air and $f_{nw} = 0.740$Hz in quiescent water. The structural damping ratio with consideration of the added mass effect was found to be $\zeta = c/(2\sqrt{k(m+m_A)}) = 2.74 \times 10^{-3}$, resulting in a low mass-damping ratio of $m^*\zeta = 7.28 \times 10^{-3}$, where $m_A = C_A m_d$ is the added mass and C_A is the added mass coefficient ($C_A = 1$ for a circular cylinder). The dynamic response of free VIV was investigated over a reduced velocity range of $2.5 < U^* < 15$, corresponding to a flow velocity range of 56mm/s $< U <$ 287mm/s and a Reynolds number range of $1450 <$ Re < 7500.

For the forced vibration experiments, the cylinder's position was controlled using a real-time feedback closed-loop motion control system. This control system employed a hardware-in-the-loop (HIL) control board (Model: Q4, Quanser Inc., Canada) embedded in a PC desktop, running on a combined software platform of MATLAB R2010a & Simulink and Real-Time Windows Target (MathWorks), and QUARC 2.1 (Quanser Inc., Canada). The motion plant consisted of a digital servo drive (Model: DPRANIE-015A400, Advanced Motion Controls, USA), a brushless DC rotary motor (Model: SM231AL-NMSN, Parker Hannifin, USA) with high resolution incremental encoder feedback device (5000 pulses per revolution or 20,000 counts per revolution post quadrature) attached to a linear ball-screw actuator (12.7mm in lead and 150mm in stroke, Model: ERS50-B02LA20-FSR150-A, Parker Hannifin, USA). The feedback control algorithm used was Proportional-Integral-Derivative (PID) algorithm [3], and the motion tracking errors were found to be within $\pm 5\mu$m ($0.0002D$).

The displacement of the cylinder was measured using a non-contact linear variable differential transformer (LVDT: SE 750-10000, Macro Sensors, USA). The lift and drag forces acting on the cylinder were measured simultaneously using a two-component force balance based on strain gauges configured in Wheatstone bridge.

The near wake flow field of the cylinder was analysed using particle image velocimetry (PIV) technique. The flow was seeded with hollow microspheres (Sphericel 110P8, Potters Industries Inc.) with a nominal diameter of 13μm and a specific weight of 1.1gcm^{-3}. Two miniature Ng:YAG pulse lasers (Continuum Minilite II Q-Switched lasers) produced a 2mm thick horizontal planar sheet, illuminating the particles in the plane of interest. Pairs of images were captured by a PCO 2000 (2048×2048pixel^2) CCD camera, equipped with a 50mm lens (Nikon Corporation, Japan). The PIV image data was analysed with in-house PIV software [6], using 32×32pixel^2 interrogation windows in a grid layout with 50% window overlap.

The PIV system's trigger TTL signal along with the cylinder position and force measurements were sampled at 1000Hz by the Q4 HIL control system. The recorded signals provided a time history of the location of the cylinder at the timing of each PIV image pair, allowing phase averaging of the PIV images based on the cylinder's position. At least 800 image pairs were taken at each U^* represented, providing approximately 200 image pairs at each of the four phases. Frequencies were extracted using FFT, and confirmed with wavelet analysis [9].

Results

Free vibration response

For close comparison with a cylinder undergoing forced oscillations, the dynamic response of the cylinder undergoing free VIV is firstly obtained. The amplitude and frequency responses of the cylinder with $m^* = 2.66$ and 2.74×10^{-3}, over a range of $2.5 < U^* < 15$, is shown in figure 2, compared with a classic case study with a similar mass ratio presented by Khalak & Williamson [11]. This comparison provides an experimental validation to ensure that the reader has confidence in the new results obtained. As expected, the response results of present case of $m^* = 2.66$ closely match the case of $m^* = 2.4$, in terms of the three-branch amplitude response pattern, the lock-in region, and the frequency response. In the initial branch, both cylinders experience extremely low-amplitude oscillations for $U^* < 3$, and then the maximum oscillation amplitude, $A^*_{\max}$, grows up sharply to above $0.4D$ as the reduced velocity is increased up to $U^* = 4.80$. As U^* is further increased, both cases undergo an amplitude response transition from the initial branch to the upper branch, and the frequency responses lock on to a frequency close to the natural frequency of the system and depart from the Strouhal number function trend, $St = f_{St}D/U$, where St is the Strouhal number, f_{St} is the vortex shedding frequency of the cylinder at rest and U is the free-stream velocity. The maximum $A^*_{\max}$ values of both cases were observed at $U^* \approx 6$. The cylinder experiences an intermittent switching transition from the upper to the lower branch at $U^* = 7.8$, which has also been seen by [11]. The lower branch is featured with very stable oscillation amplitudes of $A^*_{\max} \approx 0.6D$. In this branch, the frequency response remains remarkably constant with a value of $f^* \approx 1.342$ over a reduced velocity range of $7.6 < U^* < 10.5$. As U^* is further increased, the amplitudes gradually drop down to very low values, and the frequency responses exhibits a component following the Strouhal number functional trend, indicating end of the lock-in region.

The major difference between these two cases is the ampli-

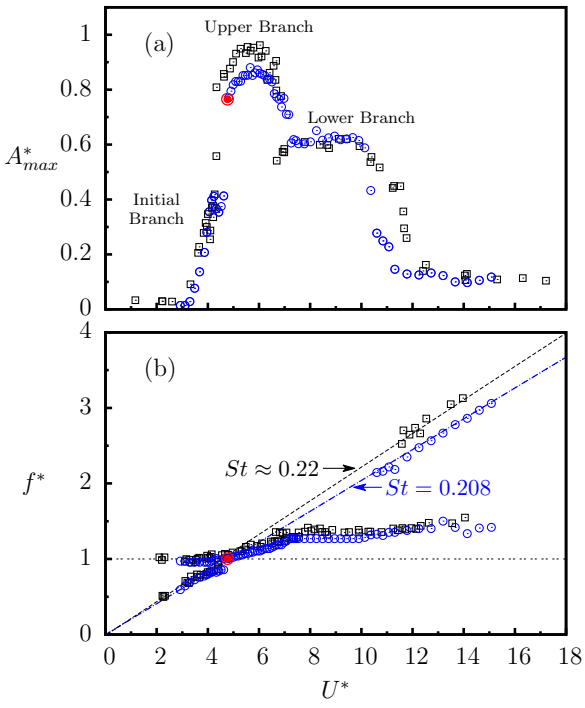

Figure 2: The amplitude and frequency responses of VIV of circular cylinders over a range of reduced velocity. (a) shows the normalised maximum amplitude response, $A^*_{max} = max(A/D)$, at each U^*, and (b) shows the normalised frequency response, $f^* = f/f_N$, where $f_N = f_{nw}$. The black squares represent the results of a cylinder with $m^* = 2.4$ and $\zeta = 4.5 \times 10^{-3}$ by [12], and the blue circles represent the present cylinder with $m^* = 2.66$ and 2.74×10^{-3}. The location of PIV measurement at $U^* = 4.93$ is highlighted by the red bull's-eye symbol.

tude magnitude of the upper branch, due to the difference in Reynolds number. The $A^*_{\max}$ peak of the present case $m^* = 2.66$ observed is $A^*_{\max} = 0.88$, approximately 12% less than that ($A^*_{\max} = 1.0$) of the case $m^* = 2.4$. The effect of Reynolds number on VIV of a circular cylinder has been well discussed in [14]; however, it is not a major focus of the investigation in this study.

Comparison between free VIV and forced tracking vibration

A direct comparison between a freely-vibrating cylinder and a VIV-trajectory-tracking cylinder is investigated at $U^* = 4.93$, as highlighted in red bull's-eye symbol in figure 2. This comparison location was at the beginning of the upper branch ($A^*_{\max} = 0.765$), where the body's oscillation frequency matched the natural frequency of the system ($f = f_{nw}$ or $f^* = 1$). Figure 3 shows the time traces of the forces and phases of both free and tracking cases. The oscillation amplitudes, shown in figure 3 (a), become much larger and more stable than in the initial branch. The time traces in figure 3 (a)-(e) show that the total lift, the vortex and the corresponding phases of both the free and tracking cases are well matched. The results of the total phase (defined as the phase angle between the transverse lift and the cylinder displacement), $\phi_{total} \approx 0^\circ$, and the vortex phase (defined as the phase angle between the vortex force and the cylinder displacement [4, 7]), $\phi_{vortex} \approx 0^\circ$ suggest the presence of $2S$ mode at this reduced velocity for the two cases. The phase-averaged results of the vorticity fields in figure 4 shows both the free and trajectory-tracking cases experience the same $2S$ mode organised in a double-row configuration. In particular, the flow structures in the very near wake of the two cases are remarkably

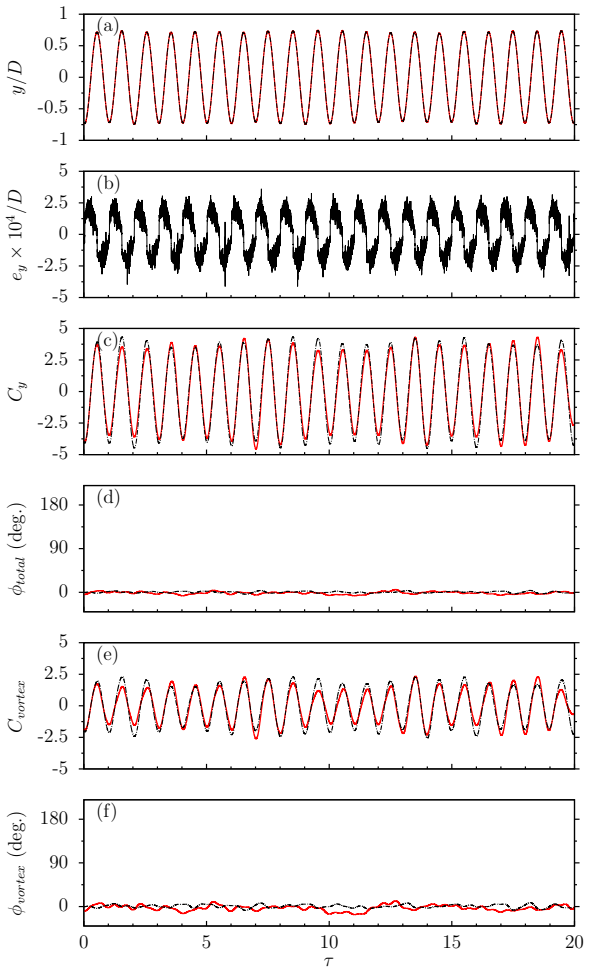

Figure 3: Time traces of the fluid forces and phases of both the freely-vibrating and trajectory-tracking cylinders at $U^* = 4.93$ and Re = 2330: (a) the body motion, (b) the position tracking errors, e_y, (c) the transverse lift coefficient, C_y, (d) the total phase, ϕ_{total}, (e) the vortex force coefficient, C_{vortex}, and (f) the vortex phase, ϕ_{vortex}. The black dot-dashed lines represent the response of freely-vibrating cylinder and the solid red lines represent the response of the tracking cylinder. Note that $\tau = t f_{nw}$ is the normalised time.

similar in all the four phases presented here. It is interesting to note how well this observation of the $2S$ mode in the upper branch agrees well with the [17]'s map of a forced-oscillating cylinder. The previous study [7] proposed that a freely-vibrating cylinder with low-$m^*\zeta$ value experienced a wake mode transition from $2S$ to $2P$ which was associated with the amplitude response jump from the initial to the upper branch, as the oscillation frequency passed through the natural frequency of the system in water. However, the present results suggest that the jump in the amplitude response from the initial to the upper branch in free vibration does not necessarily correspond to a wake mode transition from $2S$ to $2P$ mode.

Conclusions

Vortex-induced vibration of a circular cylinder with low mass and damping was experimentally investigated over a range of flow velocity. The obtained results have been validated by comparing with a classic study case in the literature. Further, the dynamic response and wake modes of the freely-vibrating cylinder located at the beginning of the upper branch have been compared directly with the VIV-trajectory-tracking cylinder.

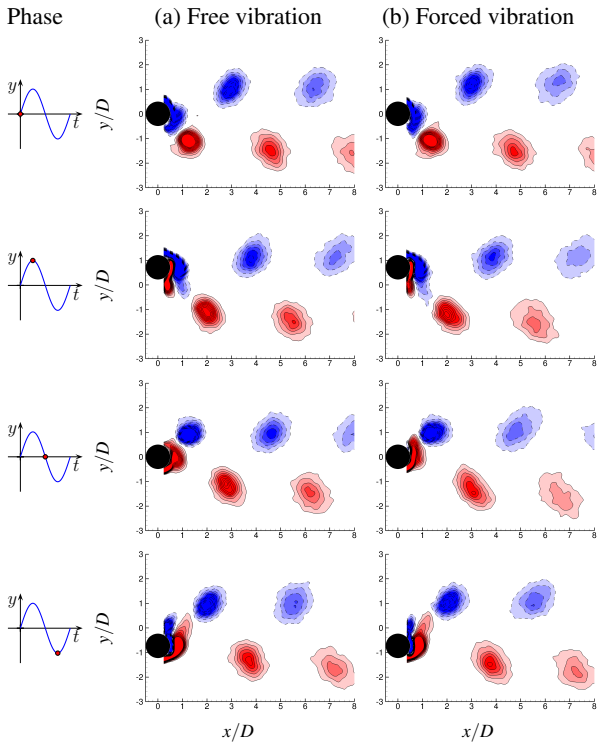

Figure 4: Phase-averaged PIV results showing the presence of 2*S* wake mode for both the freely-vibrating and trajectory-tracking cylinders at $U^* = 4.93$. The Reynolds number of both cases is $\mathrm{Re} = 2390$. Four phases are shown over one oscillation cycle. The dashed iso-lines (filled blue) represent clockwise (negative) vorticity, and the solid iso-lines (filled red) represent counter-clockwise (positive) vorticity.

This investigation firstly provided a direct close comparison between free and forced vibrations of a circular cylinder. The comparison results have shown that both the two cases exhibited highly similarities in the fluid forces and the corresponding phases, which would provide better in-depth insight into the fluid-structure interaction and the previous studies based on forced sinusoidal oscillations.

Acknowledgements

J. Zhao would like to acknowledge the support of a Monash Departmental Scholarship (MDS) from Department of Mechanical and Aerospace Engineering, Monash University, and the support from ARC Discovery (DP0774525).

References

[1] Bishop, R. E. D. and Hassan, A. Y., The lift and drag forces on a circular cylinder oscillating in a flowing fluid., *Proceedings of the Royal Society of London, series A*, **277**, 1964, 51–75.

[2] Blevins, R., *Flow-Induced Vibration*, Krieger Publishing Company, Malabar, 1990, 2nd edition edition.

[3] Callender, A., Hartree, D. and Porter, A., Time-lag in a control system, *Philosophical Transactions of the Royal Society of London. Series A, Mathematical and Physical Sciences*, **235**, 1936, 415.

[4] Carberry, J., Sheridan, J. and Rockwell, D., Controlled oscillations of a cylinder: forces and wake modes, *Journal of Fluid Mechanics*, **538**, 2005, 31–69.

[5] Feng, C., *The measurement of vortex-induced effects in flow past stationary and oscillating circular and D-section cylinders*, Master's thesis, University of British Columbia, 1968.

[6] Fouras, A., Lo Jacono, D. and Hourigan, K., Target-free stereo piv: a novel technique with inherent error estimation and improved accuracy, *Experiments in Fluids*, **44**, 2008, 317–329.

[7] Govardhan, R. and Williamson, C. H. K., Modes of vortex formation and frequency response of a freely vibrating cylinder, *Journal of Fluid Mechanics*, **420**, 2000, 85–130.

[8] Govardhan, R. and Williamson, C. H. K., Defining the modified Griffin plot in vortex-induced vibration: revealing the effect of Reynolds number using controlled damping, *Journal of Fluid Mechanics*, **561**, 2006, 147.

[9] Grinsted, A., Moore, J. C. and Jevrejeva, S., Nonlinear processes in geophysics application of the cross wavelet transform and wavelet coherence to geophysical time series, *Nonl. Procs. Geophysics*, **11**, 2004, 561–566.

[10] Khalak, A. and Williamson, C. H. K., Dynamics of a Hydroelastic Cylinder With Very Low Mass and Damping, *Journal of Fluids and Structures*, **10**, 1996, 455–472.

[11] Khalak, A. and Williamson, C. H. K., Fluid forces and dynamics of a hydroelastic structure with very low mass and damping, *Journal of Fluids and Structures*, **11**, 1997, 973–982.

[12] Khalak, A. and Williamson, C. H. K., Fluid forces and dynamics of a hydroelastic structure with very low mass and damping, *Journal of Fluids and Structures*, **11**, 1997, 973–982.

[13] Khalak, A. and Williamson, C. H. K., Motions, forces and mode transitions in vortex-induced vibrations at low mass-damping, *Journal of Fluids and Structures*, **13**, 1999, 813–851.

[14] Klamo, J., Leonard, a. and Roshko, a., The effects of damping on the amplitude and frequency response of a freely vibrating cylinder in cross-flow, *Journal of Fluids and Structures*, **22**, 2006, 845–856.

[15] Klamo, J. T., *Effects of Damping and Reynolds Number on Vortex-Induced Vibrations*, PhD thesis, California Institute of Technology, 2007.

[16] Leontini, J. S., Thompson, M. C. and Hourigan, K., Three-dimensional transition in the wake of a transversely oscillating cylinder, *Journal of Fluid Mechanics*, **577**, 2007, 79–104.

[17] Morse, T. L. and Williamson, C. H. K., Fluid forcing, wake modes, and transitions for a cylinder undergoing controlled oscillations, *Journal of Fluids and Structures*, **25**, 2009, 697–712.

[18] Naudascher, E. and Rockwell, D., *Flow-Induced Vibrations: An Engineering Guide*, Dover Publications, 2005.

[19] Williamson, C. H. K. and Roshko, A., Vortex formation in the wake of an oscillating cylinder, *Journal of Fluids and Structures*, **2**, 1988, 355–381.